

RESEARCH AND EDUCATION

## Mechanical analysis of a dental implant system under 3 contact conditions and with 2 mechanical factors



Hung-Chih Chang, MS,<sup>a</sup> Hung-Yuan Li, PhD,<sup>b</sup> Yen-Nien Chen, PhD,<sup>c</sup> Chih-Han Chang, PhD,<sup>d</sup> and Chau-Hsiang Wang, DDS, MDS, PhD<sup>e</sup>

Although dental implants have a survival rate of up to 90%,<sup>1,2</sup> failure can be devastating because of the high cost of the replacement and a healing period of up to 6 months.<sup>3,4</sup> Osseointegration has been identified as the dominant factor for the success of dental implantation.<sup>5,6</sup> However, clinical reports have indicated that the failure of dental implantation can occur even when satisfactory osseointegration has been achieved.<sup>7-9</sup> Moreover, not only the implant itself but also the abutment or screw can fracture.<sup>10-12</sup> A fractured abutment or screw might lead to damage to the implant during removal.<sup>13</sup>

The abutment-implant gap is an important issue of the conical implant system. Gehrke et al<sup>14</sup> reported that high torque values in the conical internal connection reduced the implant-abutment gap and ensured more favorable sealing ability. However, a clinical review reported that implant system failure caused by screw loosening can be up to 6%.<sup>15</sup> This loosening may increase the microgap between the abutment and implant, in

### ABSTRACT

**Statement of problem.** A unidiameter abutment attached to a large-diameter implant has been reported to result in an unexpectedly high failure rate, inconsistent with the general understanding of dental implant mechanics.

**Purpose.** The purpose of this finite element analysis study was to investigate the mechanical mechanism underlying these unexpected failures with the hypothesis that the cold welding or interference fit interface between abutment and implant increases the failure probability of a large-diameter implant system with a unidiameter abutment.

**Material and methods.** A conical implant system with different abutment gingival heights and implant diameters was analyzed for 3 contact conditions of the abutment-implant interface (bond and frictional coefficients of 0.3 and 0.7). A computer model was created using computed tomography images, and an oblique load of 100 N was applied to the abutment to determine the mechanical effect of the implant diameter and gingival height under the 3 contact conditions.

**Results.** When the abutment-implant interface was bonded, the peak stress of the abutment increased and that of the bone decreased with increasing implant diameter. When friction was applied to the abutment-implant interface, the peak stress of the implant, screw, and bone decreased with increasing implant diameter. Furthermore, the peak stress of the implant system and bone increased when the abutment gingival height increased under all contact conditions.

**Conclusions.** Cold welding or interference fit at the abutment-implant interface can prevent a screw fracture; however, it puts high stress on the unidiameter abutment neck when the implant diameter is increased. Screw loosening may lead to a slide between the abutment and implant, considerably increasing the stress of the screw. A system with a narrow diameter implant may cause an implant fracture rather than an abutment fracture when friction is applied to the abutment-implant interface. (J Prosthet Dent 2019;122:376-82)

which bacteria can accumulate.<sup>16,17</sup> Since 1999, the Morse taper design has been used to overcome possible complications caused by the microgap in the conical internal connection.<sup>18</sup> This design can increase friction between the implant and abutment or even induce cold welding to inhibit bacteria accumulation in the

<sup>a</sup>Graduate student, Department of Biomedical Engineering, National Cheng Kung University, Tainan, Taiwan Republic of China.

<sup>b</sup>Associate Professor, Department of Mold and Die Engineering, National Kaohsiung University of Science and Technology, Kaohsiung, Taiwan Republic of China.

<sup>c</sup>Postdoctoral Fellow, Department of Biomedical Engineering, National Cheng Kung University, Tainan, Taiwan Republic of China.

<sup>d</sup>Professor, Department of Biomedical Engineering, National Cheng Kung University, Tainan, Taiwan Republic of China.

<sup>e</sup>Professor, Department of Dentistry, Kaohsiung Medical University, Kaohsiung, Taiwan Republic of China.

## Clinical Implications

The high failure rate of the unidiameter abutment with a large implant size is caused by cold welding at the abutment-implant interface. Moreover, the implant system may fracture when a high abutment gingival height is used.

abutment-implant connection.<sup>19</sup> Cold welding is a bonding process in which 2 solids are forced to become a single piece by exerting a high pressure without heat.<sup>20</sup> To simplify the surgery and prosthetic processes, a unidiameter abutment design has been adopted by several implant manufacturers. However, according to a previous clinical report,<sup>21</sup> the unidiameter abutment with a large-diameter implant results in an unexpectedly high failure rate, inconsistent with the general understanding of dental implant mechanics.

In general, bending deformation is a key factor in implant system failure.<sup>22-24</sup> According to previous studies, a larger diameter implant has better stability than a smaller diameter implant to resist bending deformation and create decreased bone stress.<sup>25-29</sup> Therefore, the purpose of this study was to investigate the mechanical mechanism underlying the unexpected failure of the implant system by using finite element (FE) simulation. The research hypothesis was that the cold-welding interface increases the failure probability of a large-diameter implant system with a unidiameter abutment.

## MATERIAL AND METHODS

Images of the C-type implant system (Ankylos; Dentsply Sirona) were obtained using a microcomputed tomography ( $\mu$ CT) scanner (SkyScan 1076; Bruker MicroCT) as shown in Figure 1A. The  $\mu$ CT parameters were as follows: resolution, 35  $\mu$ m; kV/mA, 100/100; scanning angle/rotation steps, 360/1 degree; and exposure time, 474 ms. The slice images of the implant system were converted into a 3-dimensional model by using medical imaging software (Avizo 3D Software; Thermo Fisher Scientific). All material properties were assumed to be isotropic and linear elastic (Table 1).<sup>30,31</sup> FE models included an abutment, abutment screw, implant, and artificial bone block (Fig. 1B). The length of the implant and the dimension of the bone block were constant in all models. The implant was 11 mm in length, and the bone block was 25 mm in length, 15 mm in width, and 20 mm in depth. The cortical shell was assumed to have a homogeneous thickness of 2 mm (Fig. 1C). Two mechanical factors, namely the implant diameter (D) (3.5, 4.5, 5.5,

and 7 mm) and abutment gingival height (GH) (0.75, 1.5, 3, and 4.5 mm), and 3 contact conditions, namely the bond and frictional coefficients of 0.3 and 0.7, were considered to evaluate the stress of the implant system. Both frictional coefficients were included with reference to a previous study.<sup>32</sup> Subsequently, computer-aided design software (Creo Parametric; PTC) was used to modify and assemble all the models according to these factors. The configurations of all the models under different contact conditions of the implant-abutment interface are provided in Table 2.

FE software (ANSYS Workbench; ANSYS) was used to establish mesh models and to conduct computation. An oblique force of 100 N from the lingual side to the buccal side was applied to the abutment with a 45-degree inclination to the long axis of the implant. Frictionless support was applied to the distal and mesial surfaces of the cortical shell to compensate for the missing bone structure. Moreover, the distal and mesial edges of the cortical shell were fixed (Fig. 2). The implant-abutment interface was bonded to simulate the cold-welding effect exerted by the Morse taper design. Different frictional coefficients were applied to the implant-abutment interface to simulate different loosening degrees of the abutment screw. The loading and boundary conditions of the models are shown in Figure 2. The maximum principal stress was used to evaluate the stress distribution of the implant system, and the convergence test was performed by increasing the abutment mesh until the maximum principal stress of the abutment varied by less than 5%. In the convergence model, the number of elements was approximately 770 000, and the number of nodes was 460 000.

## RESULTS

The peak stress of the implant system when the abutment-implant interface was bonded is shown in Table 3. The peak stress of the abutment increased and that of the bone decreased with increasing D. In addition, the peak stress of the whole implant system and bone increased with increasing GH. The highest stress of the abutment (604.6 MPa) and implant (332.4 MPa) was located on the tension side of the abutment neck in model 16. In addition, the highest stress of the cortical bone and screw was found in model 13, and the peak bone stress (65.9 MPa) was located on the margin of the implant hole near the gingival side. The peak stress of the screw was 83.1 MPa, which occurred on the screw body near the abutment neck (Fig. 3).

The results for the peak stress of the implant system when frictional coefficients of 0.3 and 0.7 were applied to the abutment-implant interface are shown in Tables 4 and 5. Except for the abutment, the peak stress of the

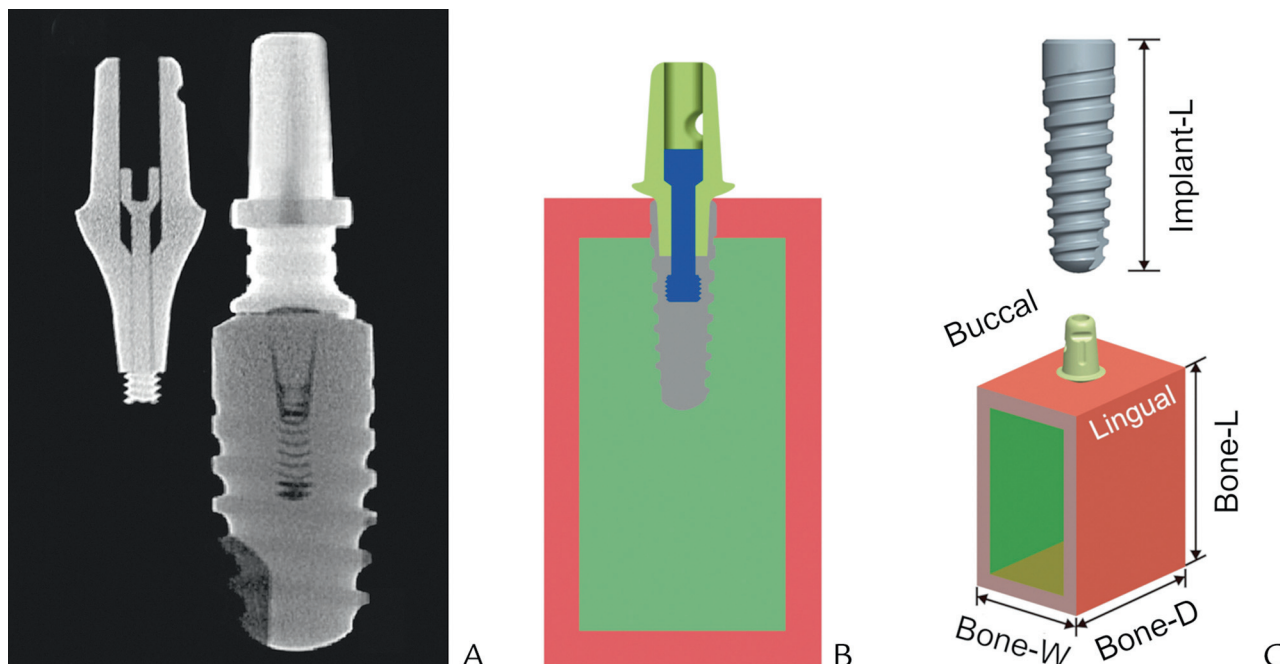


**Figure 1.** Structure of finite element model and bone block. A, Computed tomography image of abutment and implant. B, Mid-distal section of model. C, Basic information of implant system.

**Table 1.** Material properties of models

Material	Elastic Modulus (MPa)	Poisson Ratio (ν)	Reference
Titanium (implant, abutment, and screw)	110 000	0.33	Eom et al <sup>30</sup>
Cortical bone	14 000	0.3	Wang et al <sup>31</sup>
Cancellous bone	1370	0.3	Wang et al <sup>31</sup>

implant system and bone increased with a decrease in D. Similarly, the peak stress of the implant system and bone increased with increasing GH.

Regarding the stress of the implant system when the frictional coefficients of 0.7 and 0.3 were applied to the abutment-implant interface, the highest stress of the implant systems was observed in model 13. Stress values are listed in Tables 4 and 5. Changes in the frictional coefficient did not alter the mechanism of the implant system and bone, except for the implant. The peak stress was located on the neck at the tension side of the abutment, on the cortical-cancellous bone interface for the bone, and on the tension side of the screw (Fig. 4).

Regarding the stress distribution of the implant when the frictional coefficient was 0.7, the peak stress was found at the following 3 locations in different model configurations: the bottom of the abutment-implant interface on the tension side (BT), the top of the abutment-implant interface on the mid-distal side (TMD), and the top of the abutment-implant interface on the compression side (TC). When the frictional coefficient was 0.3, the peak stress of the implant was found at the

**Table 2.** Configurations of all finite element models

Test Number	Factors		Contact Situations of Implant-Abutment Interface
	Implant Diameter (mm)	Gingival Height (mm)	
1	3.5	0.75	Three contact situations including bond, frictional coefficient 0.3 and 0.7 were applied to 16 models.
2	4.5	0.75	
3	5.5	0.75	
4	7	0.75	
5	3.5	1.5	
6	4.5	1.5	
7	5.5	1.5	
8	7	1.5	
9	3.5	3	
10	4.5	3	
11	5.5	3	
12	7	3	
13	3.5	4.5	
14	4.5	4.5	
15	5.5	4.5	
16	7	4.5	

same locations as in the model with a frictional coefficient of 0.7. Furthermore, one more location of the maximum stress of the implant was observed on the bottom of the abutment-implant interface on the compression side (BC), as shown in Figure 5.

No marked differences were noted in the peak stress values of the abutment, implant, or cortical bone when different frictional coefficients were applied to the abutment-implant interface. However, the peak stress of the screw in the model with a frictional coefficient of 0.3 was

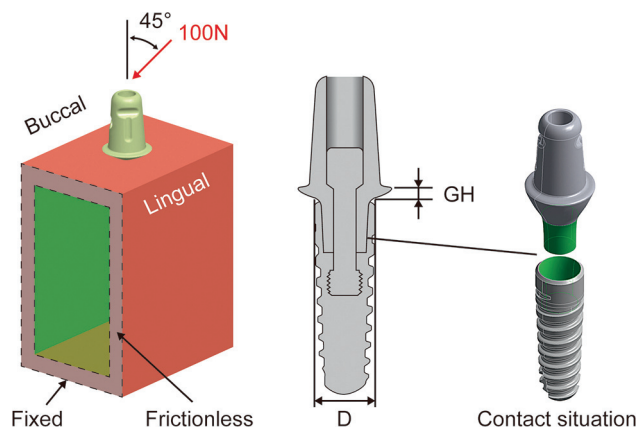


**Figure 2.** Boundary condition and control factors. D, implant diameter; GH, abutment gingival height.

higher by approximately 10% than that in the model with a frictional coefficient of 0.7.

**DISCUSSION**

The results of this study supported the hypothesis that the cold welding or interference fit interface between abutment and implant increases the failure probability of a large-diameter implant system with a unidiameter abutment. The results of FE simulation revealed that D was the dominant factor affecting the peak stress of the cortical bone in all the models. This finding is consistent with those of previous studies reporting that stress on the bone decreased with an increase in D because the large implant had larger second moments of area than did the small implant to prevent bending deformation.<sup>25-28</sup> Furthermore, this study indicated that different contact conditions at the abutment-implant interface caused different stress distribution of the abutment. The peak stress of the abutment increased with increasing D when the abutment-implant interface was bonded, which is in agreement with the results of a previous study.<sup>21</sup> This finding is because the bonding condition limits slide displacement between the abutment and implant when the implant system endures a load and enlarges the abutment deformation to compensate for the slide displacement when D increases. According to the previous study, the high torque values in the conical internal connection reduced the implant-abutment gap and ensured more favorable sealing ability.<sup>14</sup> In other words, satisfactory sealing at the implant-abutment interface can limit the slide displacement of the abutment. Although the Morse taper design is favorable for inhibiting bacteria accumulation in the abutment-implant connection,<sup>19</sup> the result of this study showed that the unidiameter abutment with a large implant may result in a crack or fracture on the abutment neck when the abutment-implant interface is bonded.

**Table 3.** Results of all finite element models when abutment-implant interface bonded

Model Number	Peak Principal Stress (MPa)			
	Abutment	Implant	Cortical Bone	Screw
1	289.3	149.8	37.1	51.7
2	308.1	155.8	21.4	50.2
3	309.9	156.7	19.0	50.7
4	320.3	162.6	12.7	51.0
5	378.3	174.0	44.2	54.9
6	403.4	181.1	23.4	53.5
7	410.9	180.8	19.8	53.7
8	426.6	200.7	14.6	53.2
9	449.1	268.9	54.2	67.9
10	489.2	253.9	27.1	65.4
11	492.7	266.5	25.0	66.0
12	534.0	266.3	16.7	66.3
13	540.6	330.4	65.9	83.1
14	588.2	322.5	35.4	80.7
15	596.8	322.5	28.5	81.3
16	604.6	332.4	17.4	81.2

When friction is applied to the implant-abutment interface, D affects the stress of the abutment screw and implant rather than the stress of the abutment. Although increasing D can slightly reduce the peak stress of the abutment, the bending stress is dominated by GH rather than D. Therefore, compared with that of GH, the effect of D on the stress distribution of the abutment is almost negligible. In addition, the stress of the implant showed a trend of convergence when D was increased from 3.5 to 7 mm under the same GH. Because the wall of the implant neck is thinner in the narrow implant than the wide implant, it may cause structural deformation and magnify the high stress of the narrow implant. A previous study indicated that the wide implant can reduce the likelihood of all component fractures in dental implant systems.<sup>29</sup>

Bending deformation is a key factor in implant failure and leads to high stress on implant systems and the bone, particularly on the abutment neck, because the initial contact point of the abutment neck is the fulcrum for the bending load.<sup>22-24</sup> In the present study, the stress of the implant system and bone increased by approximately 1.5 to 2 times when GH was increased under all contact conditions. Therefore, the bone quality of patients must be carefully evaluated before placing the implant when a conical abutment with a GH of 4.5 mm is used.

In this study, changing the frictional coefficient applied to the abutment-implant interface affected the location of the peak stress of the implant and the stress value of the screw. Under both frictional conditions, the peak stress of the implant was found at BT, TMD, and TC, which was caused by abutment rotation due to the bending force. However, the peak stress of the implant

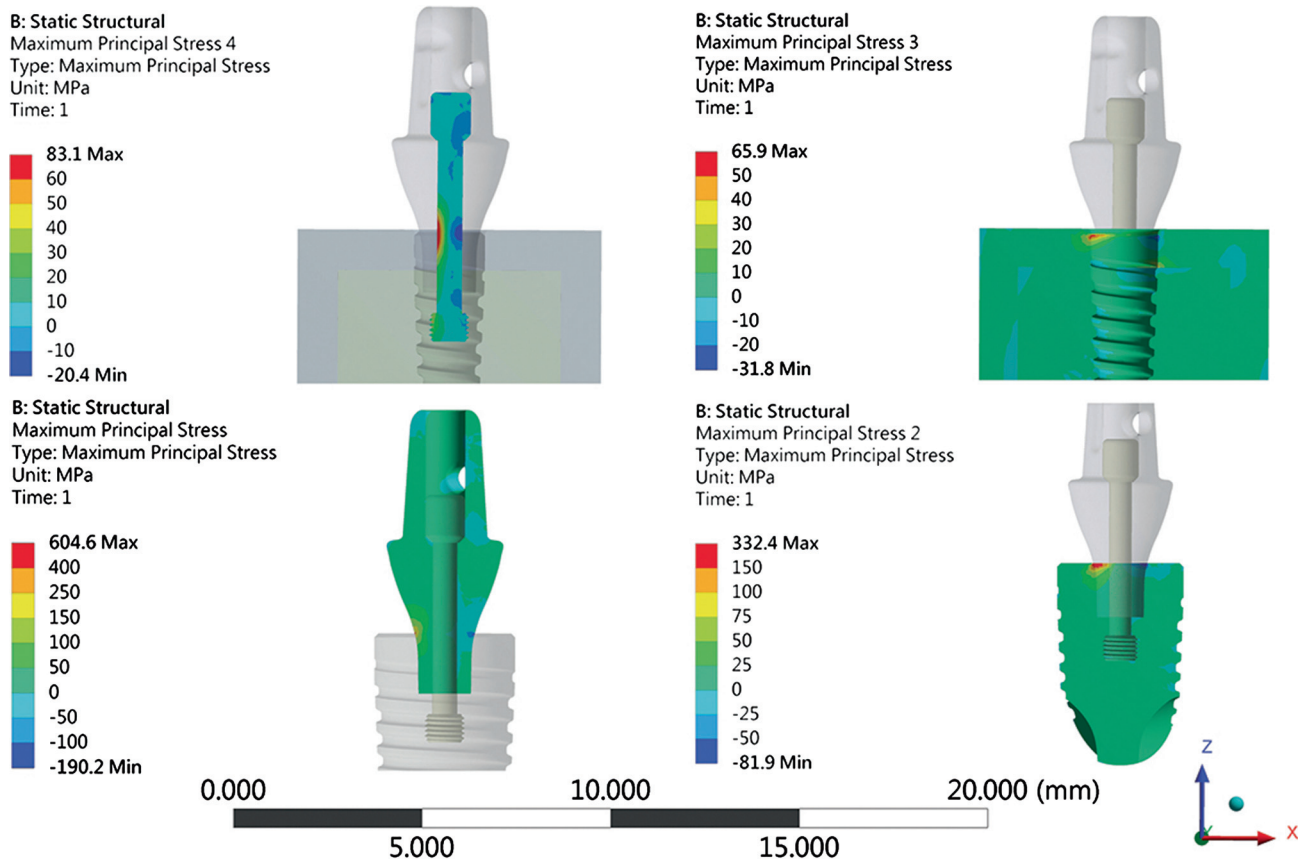


Figure 3. Maximum principal stress of implant system when abutment-implant interface bonded.

Table 4. Results of all finite element models when frictional coefficient of 0.3 applied to abutment-implant interface

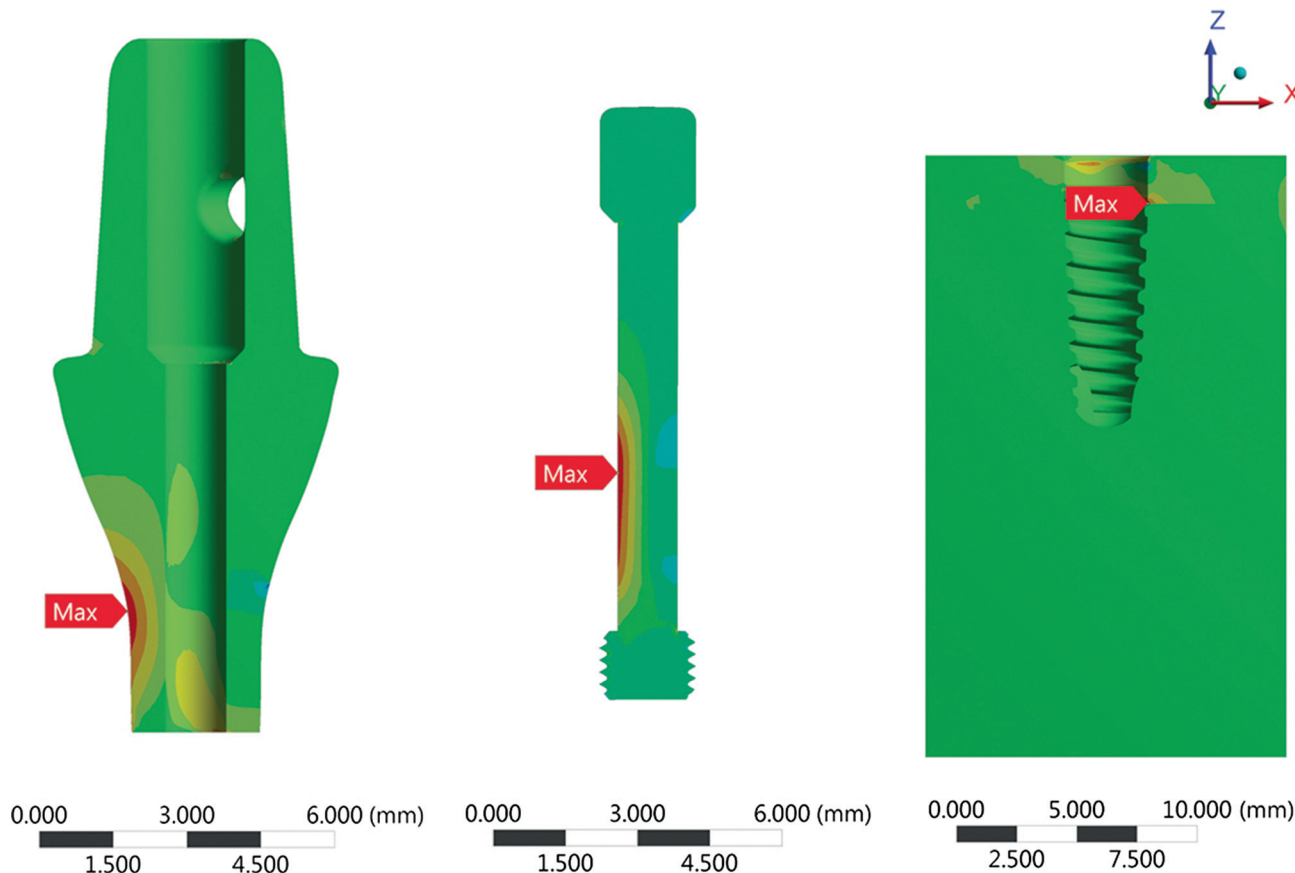
Model Number	Peak Principal Stress (MPa)			
	Abutment	Implant	Cortical Bone	Screw
1	142.6	146.4	31.6	91.2
2	137.8	97.4	23.4	70.2
3	137.6	73.6	20.4	67.0
4	137.9	63.6	13.8	65.4
5	144.8	204.5	34.6	100.8
6	141.0	101.4	25.2	84.6
7	140.8	84.3	21.4	81.2
8	139.4	66.0	15.0	79.3
9	173.7	272.8	39.3	138.3
10	163.3	134.2	29.3	113.1
11	161.1	104.9	26.9	109.1
12	160.4	88.7	17.5	106.8
13	222.6	351.1	45.2	183.4
14	209.7	162.4	33.6	140.9
15	207.1	136.7	29.7	136.2
16	206.2	115.4	19.4	133.2

Table 5. Results of all finite element models when frictional coefficient of 0.7 applied to abutment-implant interface

Model Number	Peak Principal Stress (MPa)			
	Abutment	Implant	Cortical Bone	Screw
1	138.8	157.0	32.1	74.6
2	135.3	105.9	23.0	65.7
3	135.0	85.7	20.2	63.3
4	135.1	82.2	13.6	62.3
5	139.5	208.7	35.5	87.9
6	137.2	118.2	25.2	77.9
7	137.1	94.8	21.1	74.9
8	135.7	89.1	14.7	73.2
9	164.1	273.6	40.4	115.1
10	156.3	146.8	29.2	101.9
11	155.4	123.2	26.4	99.0
12	155.3	105.4	17.0	97.2
13	210.9	343.2	46.5	141.5
14	201.0	182.8	33.4	126.1
15	200.0	156.7	29.0	122.7
16	199.8	134.2	18.8	120.4

located on BC was found only in the model with a frictional coefficient of 0.3. According to the friction equation, the axial displacement of the abutment increased when the frictional coefficients of the abutment-implant

interface decreased. This results in a high stress concentration at BC when the abutment undergoes deformation. Although the frictional coefficients of the abutment-implant interface could change the peak stress



**Figure 4.** Maximum principal stress of abutment, screw, and bone when abutment-implant interface assigned frictional coefficients of 0.7 and 0.3.

position of the implant in this study, the peak stress of all implants was lower than that of the abutment, except for the implant with a D of 3.5 mm. When friction was applied to the abutment-implant interface, the stress of the implant with a D of 3.5 mm was higher than that of the other components; this may cause a fracture in the implant body rather than in the other components when the implant system is under an ultimate load. This result is consistent with a previous study.<sup>12</sup>

The peak stress of the screw occurred on the tension side in all the models and increased with a decrease in the frictional coefficient applied to the abutment-implant interface. Furthermore, the stress of the screw increased by approximately 2 times when the abutment-implant interface changed from bond to friction; this resulted in the stress of the screw being in the same order as that of the abutment and implant. Although the stress of all screws was lower than that of the abutment in this study, screw fractures were reported in all cases of abutment fractures in previous studies.<sup>21,12</sup>

This study has limitations. A conical abutment was used to investigate stress distribution under various factors and contact conditions. However, some of the results of this study were obtained using only a conical implant system with a unidiameter abutment. In

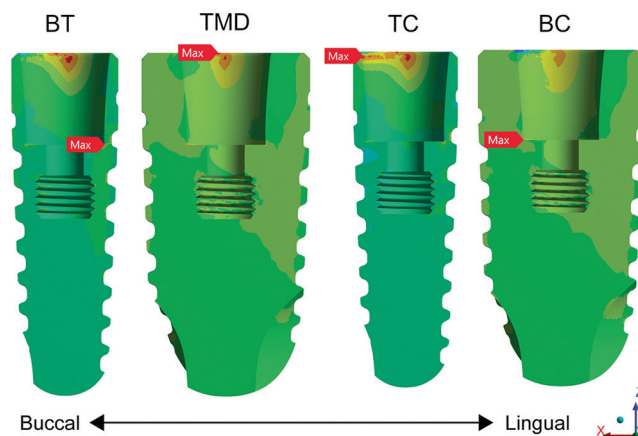


**Figure 5.** Maximum stress of implant when abutment-implant interface assigned frictional coefficients of 0.7 and 0.3. BC, bottom of abutment-implant interface on compression side; BT, bottom of abutment-implant interface on tension side; TC, top of abutment-implant interface on compression side; TMD, top of abutment-implant interface on mid-distal side.

addition, the varying crown geometry of different patients may weakly affect the stress distribution of the implant system. However, to determine the mechanism of the implant system without considering any individual

factor, this study excluded the crown structure in all the models.

## CONCLUSIONS

Within the limitations of this FE analysis study, the following conclusions were drawn:

1. Cold welding or interference fit at the abutment-implant interface can prevent screw fracture; however, it can lead to a high stress concentration on the unidiameter abutment when the diameter is increased.
2. Screw loosening may lead to a slide between the abutment and implant, which can considerably increase the stress in the screw. This may lead to screw fracture after an abutment fracture when the implant system endures ultimate and cyclic loading.
3. When friction is applied to the abutment-implant interface of an implant with a diameter of 3.5 mm, an implant fracture rather than an abutment or screw fracture may occur.
4. Gingival height is the dominant factor affecting the peak stress of the implant system and bone. The bone quality of patients must be carefully evaluated before placing an implant when an abutment with a high gingival height is used. Moreover, implant diameter is the crucial factor affecting the stress of the bone under all contact conditions, and the bone stress decreases when the diameter is increased.

## REFERENCES

1. De Angelis F, Papi P, Mencio F, Rosella D, Di Carlo S, Pompa G. Implant survival and success rates in patients with risk factors: results from a long-term retrospective study with a 10 to 18 years follow-up. *Eur Rev Med Pharmacol Sci* 2017;21:433-7.
2. Lee CT, Chen YW, Starr JR, Chuang SK. Survival analysis of wide dental implant: systematic review and meta-analysis. *Clin Oral Implants Res* 2016;27:1251-64.
3. Dang Y, Zhang L, Song W, Chang B, Han T, Zhang Y, et al. In vivo osseointegration of Ti implants with a strontium-containing nanotubular coating. *Int J Nanomedicine* 2016;11:1003-11.
4. Nedir R, Bischof M, Szmukler-Moncler S, Bernard JP, Samson J. Predicting osseointegration by means of implant primary stability. *Clin Oral Implants Res* 2004;15:520-8.
5. Brånemark PI, Adell R, Breine U, Hansson BO, Lindström J, Ohlsson A. Intra-osseous anchorage of dental prostheses: I. Experimental Studies. *Scand J Plast Reconstr Surg* 1969;3:81-100.
6. Albrektsson T, Brånemark PI, Hansson HA, Lindström J. Osseointegrated titanium implants. Requirements for ensuring a long-lasting, direct bone-to-implant anchorage in man. *Acta Orthop Scand* 1981;52:155-70.
7. Gealh WC, Mazzo V, Barbi F, Camarini ET. Osseointegrated implant fracture: causes and treatment. *J Oral Implantol* 2011;37:499-503.
8. Luterbacher S, Fourmousis I, Lang NP, Brägger U. Fractured prosthetic abutments in osseointegrated implants: a technical complication to cope with. *Clin Oral Implants Res* 2000;11:163-70.
9. Walia MS, Arora S, Luthra R, Walia PK. Removal of fractured dental implant screw using a new technique: a case report. *J Oral Implantol* 2012;38:747-50.
10. Freitas-Júnior AC, Almeida EO, Bonfante EA, Silva NR, Coelho PG. Reliability and failure modes of internal conical dental implant connections. *Clin Oral Implants Res* 2013;24:197-202.
11. Nergiz I, Schmage P, Shahin R. Removal of a fractured implant abutment screw: a clinical report. *J Prosthet Dent* 2004;91:513-7.
12. Shemtov-Yona K, Rittel D, Machtei EE, Levin L. Effect of dental implant diameter on fatigue performance. Part II: failure analysis. *Clin Implant Dent Relat Res* 2014;16:178-84.
13. Taira Y, Sawase T. A modified technique for removing a failed abutment screw from an implant with a custom guide tube. *J Oral Implantol* 2012;38:165-9.
14. Gehrke SA, Shibli JA, Aramburú Junior JS, de Val JE, Calvo-Girardo JL, Dedavid BA. Effects of different torque levels on the implant-abutment interface in a conical internal connection. *Braz Oral Res* 2016;30:e40.
15. Goodacre CJ, Bernal G, Rungcharassaeng K, Kan JY. Clinical complications with implants and implant prostheses. *J Prosthet Dent* 2013;90:121-32.
16. Brogini N, McManus LM, Hermann JS, Medina RU, Oates TW, Schenk RK, et al. Persistent acute inflammation at the implant-abutment interface. *J Dent Res* 2003;82:232-7.
17. Lopes de Chaves E Mello Dias EC, Sperandio M, Napimoga MH. Association between implant-abutment microgap and implant circularity to bacterial leakage: an in vitro study using tapered connection implants. *Int J Oral Maxillofac Implants* 2018;33:505-11.
18. Scacchi M, Merz BR, Schär AR. The development of the ITI dental implant system. Part 2: 1998-2000: steps into the next millennium. *Clin Oral Implants Res* 2000;11:22-32.
19. Dibart S, Warbington M, MingFan S, Skobe Z. In vitro evaluation of the implant-abutment bacterial seal: the locking taper system. *Int J Oral Maxillofac Implants* 2005;20:732-7.
20. Lu Y, Huang JY, Wang C, Sun S, Lou J. Cold welding of ultrathin gold nanowires. *Nat Nanotechnol* 2010;5:218-24.
21. Shim HW, Yang BE. Long-term cumulative survival and mechanical complications of single-tooth Ankylos implants: focus on the abutment neck fractures. *J Adv Prosthodont* 2015;7:423-30.
22. Rangert B, Krogh PH, Langer B, Van Roekel N. Bending overload and implant fracture: a retrospective clinical analysis. *Int J Oral Maxillofac Implants* 1995;10:326-34.
23. Suzuki H, Hata Y, Watanabe F. Implant fracture under dynamic fatigue loading: influence of embedded angle and depth of implant. *Odontology* 2016;104:357-62.
24. Wang CF, Huang HL, Lin DJ, Shen YW, Fuh LJ, Hsu JT. Comparisons of maximum deformation and failure forces at the implant-abutment interface of titanium implants between titanium-alloy and zirconia abutments with two levels of marginal bone loss. *Biomed Eng Online* 2013;12:45.
25. Hsu J, Fuh L, Lin D, Shen Y, Huang H. Bone strain and interfacial sliding analyses of platform switching and implant diameter on an immediately loaded implant: experimental and three-dimensional finite element analyses. *J Periodontol* 2009;80:1125-32.
26. Misch CE. *Dental implant prosthetics*. 2nd ed. St. Louis, MO: Elsevier Health Sciences; 2014. p. 294-314.
27. Baggi L, Cappelloni I, Di Girolamo M, Maceri F, Vairo G. The influence of implant diameter and length on stress distribution of osseointegrated implants related to crestal bone geometry: a three-dimensional finite element analysis. *J Prosthet Dent* 2008;100:422-31.
28. Himmlová L, Dostálová T, Kácvovský A, Konvícková S. Influence of implant length, diameter on stress distribution: a finite element analysis. *J Prosthet Dent* 2004;91:20-5.
29. Boggan RS, Strong JT, Misch CE, Bidez MW. Influence of hex geometry and prosthetic table width on static and fatigue strength of dental implants. *J Prosthet Dent* 1999;82:436-40.
30. Eom JW, Lim YJ, Kim MJ, Kwon HB. Three-dimensional finite element analysis of implant-assisted removable partial dentures. *J Prosthet Dent* 2017;117:735-42.
31. Wang CH, Du JK, Li HY, Chang HC, Chen KK. Factorial analysis of variables influencing mechanical characteristics of a post used to restore a root filled premolar using the finite element stress analysis combined with the Taguchi method. *Int Endod J* 2016;49:690-9.
32. Bozkaya D, Müftü S. Mechanics of the taper integrated screwed-in (TIS) abutments used in dental implants. *J Biomech* 2005;38:87-97.

### Corresponding author:

Dr Chau-Hsiang Wang  
Department of Dentistry, Kaohsiung Medical University Hospital  
No.100, Shih-Chuan 1st Road  
Kaohsiung, 807  
TAIWAN, REPUBLIC OF CHINA  
Email: chhsua@kmu.edu.tw

Copyright © 2018 by the Editorial Council for *The Journal of Prosthetic Dentistry*.  
<https://doi.org/10.1016/j.prosdent.2018.10.008>